Journal of Medicinal Chemistry Article

J. Med. Chem. **2010,** *53,* 723–733 **723**
DOI: 10.1021/jm901269y

Novel Ester and Acid Derivatives of the 1,5-Diarylpyrrole Scaffold as Anti-Inflammatory and Analgesic Agents. Synthesis and in Vitro and in Vivo Biological Evaluation

Mariangela Biava,*[,†] Giulio C. Porretta,[†] Giovanna Poce,[†] Claudio Battilocchio,[†] Fabrizio Manetti,*[,‡] Maurizio Botta,[‡] Stefano Forli,[‡,○] Lidia Sautebin,[∥] Antonietta Rossi,[⊥] Carlo Pergola,[∥] Carla Ghelardini,[@] Nicoletta Galeotti,[@] Francesco Makovec,[#] Antonio Giordani,[#] Paola Anzellotti,[▽] Paola Patrignani,[▽] and Maurizio Anzini[‡,§]

[†]*Dipartimento di Studi di Chimica e Tecnologie del Farmaco, Università "La Sapienza", piazzale Aldo Moro 5, I-00185 Roma, Italy,* [‡]*Dipartimento Farmaco Chimico Tecnologico, Università degli Studi di Siena, via Alcide de Gasperi 2, I-53100 Siena, Italy,* [§]*European Research Centre for Drug Discovery and Development, via Banchi di Sotto 55, I-53100 Siena, Italy,* [∥]*Dipartimento di Farmacologia Sperimentale, Università di Napoli "Federico II", via D. Montesano 49, I-80131 Napoli, Italy,* [⊥]*IRCCS Centro Neurolesi "Bonino-Pulejo", via Provinciale Palermo, C. da Casazza, I-98124 Messina, Italy,* [@]*Dipartimento di Farmacologia, Università di Firenze, viale G. Pieraccini 6, I-50139 Firenze, Italy,* [#]*Rottapharm SpA, via Valosa di Sopra 7, I-20052 Monza, Italy, and* [▽]*Department of Medicine and Center of Excellence on Aging, "G. d'Annunzio" University and CeSI, Via dei Vestini 31, I-66013 Chieti, Italy.* [○]*Present address: Department of Molecular Biology, MB-5, The Scripps Research Institute, 10550 N. Torrey Pines Rd., La Jolla, CA 92037-1000.*

Received August 25, 2009

A new generation of selective cyclooxygenase-2 (COX-2) inhibitors (coxibs) was developed to circumvent the major side effects of cyclooxygenase-1 (COX-1) and COX-2 inhibitors (stomach ulceration and nephrotoxicity). As a consequence, coxibs are extremely valuable in treating acute and chronic inflammatory conditions. However, the use of coxibs, such as rofecoxib (Vioxx), was discontinued because of the high risk of cardiovascular adverse events. More recent clinical findings highlighted how the cardiovascular toxicity of coxibs could be mitigated by an appropriate COX-1 versus COX-2 selectivity. We previously reported a set of substituted 1,5-diarylpyrrole derivatives, selective for COX-2. Here, we describe the synthesis of new 1,5-diarylpyrroles along with their inhibitory effects in vitro, ex vivo, and in vivo toward COX isoenzymes and their analgesic activity. Isopropyl-2-methyl-5-[4-(methylsulfonyl)phenyl]-1-phenyl-1*H*-pyrrole-3-acetate (**10a**), a representative member of the series, was selected for pharmacokinetic and metabolic studies.

Introduction

Selective COX-2 inhibitors were developed to reduce gastrointestinal (GI)[a] side effects associated with the use of traditional nonsteroidal anti-inflammatory drugs (tNSAIDs).[1,2] A reduced incidence of serious GI adverse effects compared to tNSAIDs has been demonstrated for two highly selective COX-2 inhibitors (namely, rofecoxib and lumiracoxib) in large randomized clinical trials.[3,4] This was a proof of concept that sparing COX-1 in the GI tract and possibly in platelets translates into a safer GI profile.[5] Some coxibs, such as rofecoxib and valdecoxib, were withdrawn from the market because of an increased incidence of thrombotic events presumably associated with selective inhibition of COX-2-dependent generation of prostacyclin in endothelial cells, without the concomitant complete suppression of COX-1-dependent platelet thromboxane (TX) A_2 generation.[6] Furthermore, the European Medicines Agency (EMEA) has recommended the withdrawal of the marketing authorizations for all lumiracoxib-containing medicines, because of the risk of serious side effects affecting the liver.[7]

In vitro selectivity toward COX-2 is described as the ratio of the concentration required to inhibit the activity of the isoenzymes by 50% (IC_{50} toward COX-1/IC_{50} toward COX-2).[8] Selectivity at the circulating drug concentration impacts both efficacy and side effects. It was shown that, among tNSAIDs, there is a cluster of compounds, such as etodolac[9] (**2a**), meloxicam[10] (**3**), nimesulide[11] (**4**), and diclofenac[12] (**5**) (Chart 1), that are 5−29-fold more potent in vitro toward COX-2, in comparison to COX-1. Among coxibs, rofecoxib[13] (**1a**), celecoxib[14] (**1b**), valdecoxib[15] (**1c**), etoricoxib[16] (**1d**), and lumiracoxib[17] (**1e**) (Chart 1) showed a wide range of COX-1/COX-2 IC_{50} ratio values (from 30 for **1b** to 433 for **1e**).

In the in vitro human whole blood (HWB) assay, the biochemical selectivity of COX inhibitors is a continuous variable.[18,19] It is worth mentioning that 80% ex vivo inhibition of COX-2 (in whole blood) by circulating drug concentrations seems to be sufficient to translate into efficacy (analgesia).[20]

Moreover, a high degree of COX-2 inhibition seems to be associated with an increased incidence of cardiovascular events (with myocardial infarction that exceeds over stroke), and such an effect could be mitigated by an appropriate

*To whom correspondence should be addressed. M. Biava: phone, +39 06 49913812; fax, +39 06 49913133; e-mail, mariangela.biava@uniroma1.it. F. Manetti: phone, +39 0577 234330; fax, +39 0577 234333; e-mail, manettif@unisi.it.

[a] Abbreviations: NSAIDs, nonsteroidal anti-inflammatory drugs; COX, cyclooxygenase; AA, arachidonic acid; PGH_2, prostaglandin H_2; PGE_2, prostaglandin E_2; HWB, human whole blood; tNSAIDs, traditional nonsteroidal anti-inflammatory drugs; GI, gastrointestinal; CV, cardiovascular; DMEM, Dulbecco's modified Eagle's medium; FBS, fetal bovine serum; LPS, lipopolysaccharide; RIA, radioimmunoassay; TX, thromboxane; MPE, maximum percent effect; CMC, carboxymethylcellulose; MSMS, maximal speed molecular surface.

Published on Web 12/03/2009

Chart 1. Structure of NSAIDs, Including Coxib Derivatives, Traditional NSAIDs, and Previously Described Pyrrole Compounds

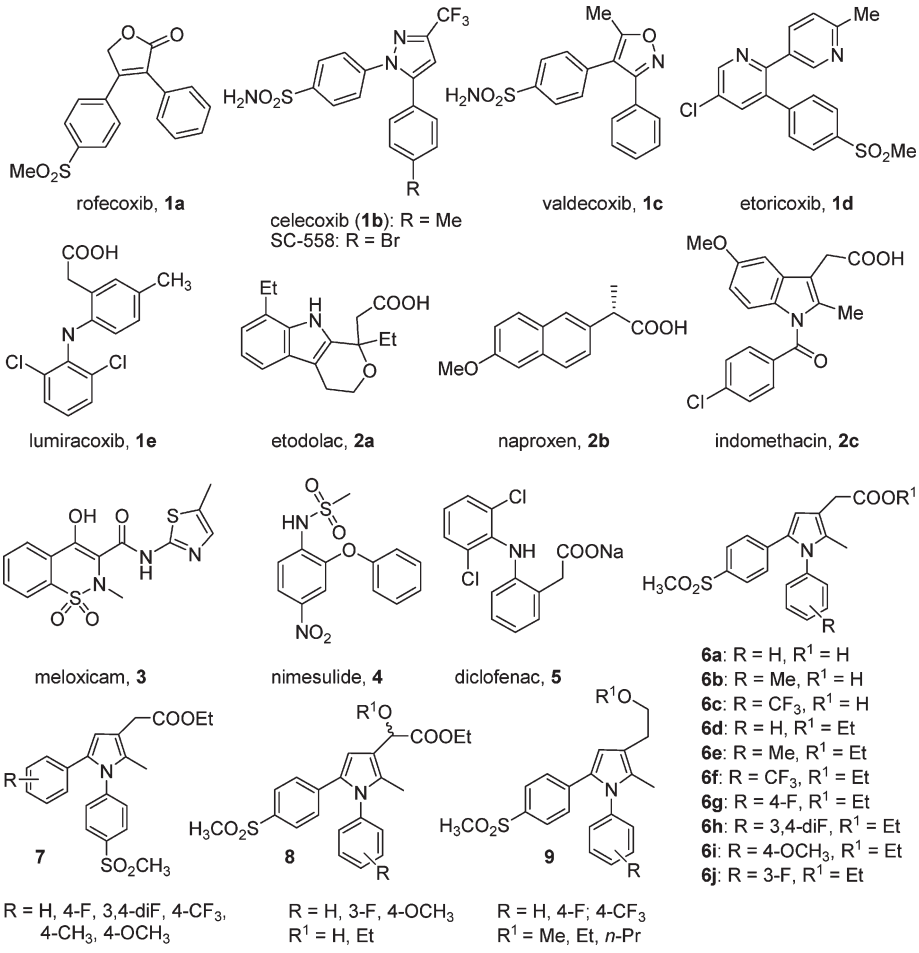

inhibition of platelet COX-1 activity (i.e., > 95%, necessary to inhibit platelet function).[6,18] Accordingly, the fact that most tNSAIDs and coxibs are selective in vivo for COX-2 at therapeutic doses could account for their thrombogenic effects.[21,22] Conversely, an incomplete inhibition of COX-2 in the kidney might attenuate the deleterious functional effect derived from the lack of COX-2-dependent prostacyclin.[6,22] Thus, selective and profound inhibition of COX-2 by coxibs may have a greater propensity to increase side effects than balanced inhibition of both COX-1 and COX-2 by tNSAIDs.

In addition, the approach to identifying biochemical and/or genetic biomarkers to select the patients who are most susceptible to a hazard or benefit by selective inhibition of COX-2 should be taken into account as well.[5,9] In fact, a marked intersubject variability in COX-2 inhibition by NSAIDs, in part due to a genetic background, has been shown.[10,11]

Despite the fact that several NSAIDs with suitable pharmacodynamic features are available (e.g., **3**−**5**), most of them have short half-life, which leads to their administration at high doses (often overshooting) to extend the pharmacodynamic effects, and in addition, some of them displayed hepatic toxicity (i.e., **5**).

We have previously reported design, synthesis, and anti-inflammatory properties of a class of novel pyrrole-containing anti-inflammatory agents.[23−27] In particular, we focused our attention on the synthesis of 1,5-diarylpyrrole-3-acetic acids, esters, α-hydroxy esters, and ethers **6**−**9** (Chart 1) as new COX-2 selective inhibitors in which the pyrroleacetic and vicinal diaryl heterocyclic moieties were reminiscent both of the "coxib" family **1a**−**e** cited above and of indomethacin (**2c**), respectively. A structure−activity relationship (SAR) analysis of such compounds, supported by molecular docking simulations of these inhibitors within the COX-2 binding site,[23−26] allowed us to rule out several considerations. (i) The position of the *p*-methylsulfonyl substituent was very important for activity (compounds **6** being more active than **7**). (ii) Surprisingly, the acetic ester chain at C3 of the pyrrole ring led to compounds more active than the corresponding acids.[23,24,26] (iii) Substituents and the substitution pattern on the phenyl ring at N1 influenced activity in the following order: 3-F = 4-F > 3,4-diF > 4-OMe > H > 4-CF_3 > 4-CH_3.[23−27]

In this paper, we report the synthesis and biological activity of new derivatives **10a**−**h** (Scheme 1 and Table 1), in which longer side chains were introduced at C3 on the basis of the hypothesis that such chains could better interact with hydrophobic residues of the carboxylate pocket of the receptor.[23−26] In particular, compounds **10a**−**h**, bearing an isopropyl and an *n*-butyl ester function, a N1 phenyl ring with various substituents previously found to be important for activity (namely, 3-F, 3,4-diF, and 4-OCH_3), and a C5 *p*-methylsulfonyl phenyl moiety, showed outstanding activity. The new compounds were evaluated in vitro for their ability to inhibit COX-1 and COX-2 in a J774 murine macrophage cell line, and biochemical data were rationalized through docking simulations. In addition, their inhibitory effects on platelet COX-1 and monocyte COX-2 activity were compared in an in vitro HWB assay.[18,19] Their in vivo anti-inflammatory and analgesic

Scheme 1[a]

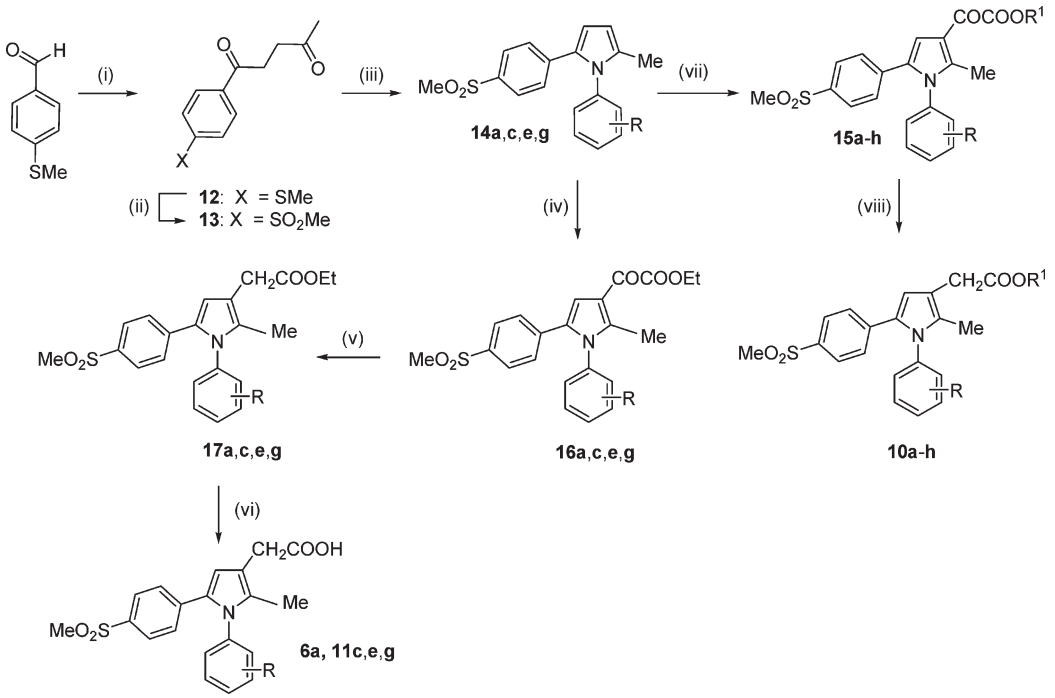

[a] Compounds: **10a**, R = H, R^1 = isopropyl, 55% yield; **10b**, R = H, R^1 = *n*-butyl, 50% yield; **10c**, R = 3-F, R^1 = isopropyl, 96% yield; **10d**, R = 3-F, R^1 = *n*-butyl, 40% yield; **10e**, R = 3,4-diF, R^1 = isopropyl, 45% yield; **10f**, R = 3,4-diF, R^1 = *n*-butyl, 40% yield; **10g**, R = 4-OCH_3, R^1 = isopropyl, 40% yield; **10h**, R = 4-OCH_3, R^1 = *n*-butyl, 40% yield; **6a**, R = H, 71% yield; **11c**, R = 3-F, 60% yield; **11e**, R = 3,4-diF, 75% yield; **11g**, R = 4-OCH_3, 70% yield; **14a**, R = H, 80% yield; **14c**, R = 3-F, 80% yield; **14e**, R = 3,4-diF, 74% yield; **14g**, R = 4-OCH_3, 70% yield; **15a**, R = H, R^1 = isopropyl, 76% yield; **15b**, R = H, R^1 = *n*-butyl, 90% yield; **15c**, R = 3-F, R^1 = isopropyl, 40% yield; **15d**, R = 3-F, R^1 = *n*-butyl, 55% yield; **15e**, R = 3,4-diF, R^1 = isopropyl, 77% yield; **15f**, R = 3,4-diF, R^1 = *n*-butyl, 65% yield; **15g**, R = 4-OCH_3, R^1 = isopropyl, 40% yield; **15h**, R = 4-OCH_3, R^1 = *n*-butyl, 60% yield; **16a**, R = H, 76% yield; **16c**, R = 3-F, 57% yield; **16e**, R = 3,4-diF, 77% yield; **16g**, R = 4-OCH_3, 75% yield; **17a**, R = H, 71% yield; **17c**, R = 3-F, 45% yield; **17e**, R = 3,4-diF, 60% yield; **17g**, R = 4-OCH_3, 30% yield. Reagents and conditions: (i) CH_2=CHCOMe, TEA, 3-ethyl-5-(2-hydroxyethyl)-4-methylthiazolium bromide, MW, 15 min; (ii) Oxone, MeOH/H_2O, room temperature, 2 h; (iii) RPhNH_2, *p*-toluenesulfonic acid, EtOH, MW, 45 min; (iv) EtOCOCOCl, $TiCl_4$, CH_2Cl_2, room temperature, 4 h; (v) Et_3SiH, TFA, room temperature, 2 h; (vi) 1 N NaOH, MeOH, 1 h; (vii) ClCOCOCl, 2,6-lutidine, CH_2Cl_2, R^1OH; (viii) Et_3SiH, TFA, room temperature, 2 h.

Table 1. In Vitro Inhibition (J774 murine macrophage assay) of COX-1 and COX-2 by Compounds **6a,d**, **10a−h**, and **11c,e,g**, and Celecoxib

	IC_{50} (μM)[a]		COX-2 inhibition (%)		
compd	COX-1	COX-2	10 μM	1 μM	selectivity index[b]
10a	> 100	0.0073	100	100	> 13600
10b	> 100	0.014	88	85	> 7100
10c	> 100	0.043	91	85	> 2300
10d	> 100	0.024	100	87	> 4100
10e	> 100	0.021	90	85	> 4700
10f	> 100	0.030	90	86	> 3300
10g	> 100	0.022	100	88	> 4500
10h	> 100	0.038	92	89	> 2600
6a[c]	> 100	1.0	100	43	> 100
11c	> 100	0.028	96	89	> 3500
11e	10	0.26	98	70	38
11g	> 100	0.17	90	62	> 580
6d[c]	> 100	0.04	84	79	> 2500
celecoxib, **1b**	5.1	0.079	95	80	65

[a] Results are expressed as the mean (n = 3) of the % inhibition of PGE_2 production by test compounds with respect to control samples. [b] In vitro COX-2 selectivity index [$IC_{50(COX\text{-}1)}/IC_{50(COX\text{-}2)}$]. [c] See ref 23.

activity was also evaluated in several animal models. A representative member of the series (**10a**) was selected to perform pharmacokinetic studies. After both oral and intravenous administrations of **10a**, the formation of the corresponding acid **6a** was observed. Accordingly, considering that the ester derivatives could give rise in vivo to the formation of corresponding acids, the anti-inflammatory and analgesic activities of acid derivatives **6a** and **11c,e,g** were also evaluated, using the same protocols applied for the corresponding esters.

Chemistry

The synthesis of the target compounds is described in Scheme 1. Briefly, the reaction of 4-(methylthio)benzaldehyde with methyl vinyl ketone for 15 min using the microwave apparatus gave the intermediate **12**,[28] which was transformed into the corresponding 4-methylsulfonyl derivative **13** by means of Oxone oxidation.[29] Next, following the Paal−Knoor condensation in the presence of the appropriate arylamine (45 min by using the microwave apparatus),[28] **13** cyclized to yield the expected 1,5-diarylpyrroles **14a,c,e,g**. The construction of the C3 side chain was achieved by regioselective acylation of **14a,c,e,g** with oxalyl chloride in the presence of 2,6-lutidine to give corresponding α-keto acid chlorides that, by the successive reaction in the presence of the proper alcohol, gave the corresponding α-keto ester derivatives **15a−h** in a one-pot reaction. Compounds **15a−h** were in turn reduced by means of triethylsilane in trifluoroacetic acid to give the pyrrole esters **10a−h**.[30] Construction of the C3 acetic acid chain of **6a** and **11c,e,g** was achieved by regioselective acylation of **14a,c,e,g** with ethoxalyl chloride in the presence of titanium tetrachloride to give corresponding α-keto esters **16a,c,e,g** in turn reduced (triethylsilane in trifluoroacetic acid)

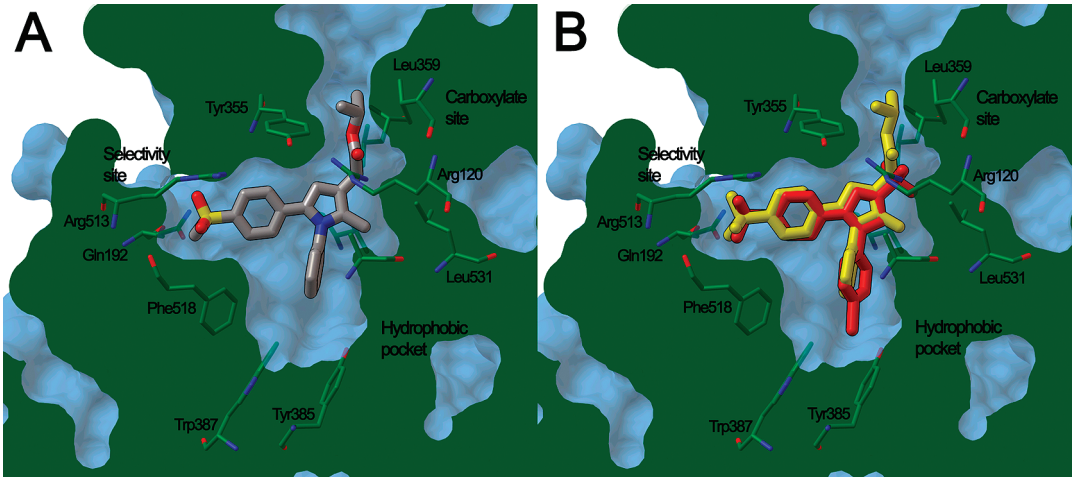

Figure 1. Graphical representation of the binding mode of **10a** within the COX-2 binding site (A), in comparison to the cocrystallized inhibitor SC-558 (B) (SC-558, red; **10a**, yellow). For the sake of clarity, only the most important residues flanking the binding site are shown as thin lines. Images have been generated by means of ADT version 1.5.1.

to the pyrrole acetic esters **17a,c,e,g** that led to the corresponding acids **6a** and **11a,c,e,g** by treatment with 1 N NaOH in MeOH for 1 h.

Results and Discussion

Previous molecular docking simulations, in combination with GRID calculations, led us to hypothesize the binding mode of 1,5-diarylpyrrole derivatives within the COX-2 binding site and to identify the interactions between ligands and the protein that allowed us to account for the major SARs. In particular, the docked orientation of pyrroles showed the N1 phenyl ring, the C3 side chain, and the C5 phenyl ring embedded in the hydrophobic pocket, the carboxylate site, and the selectivity site of the enzyme, respectively (Figure 1A), in correspondence with the bromophenyl moiety, the trifluoromethyl group, and the N1 phenyl ring of the cocrystallized inhibitor SC-558, respectively (Figure 1B). The structure of SC-558 is depicted in Chart 1. Moreover, the identification of points of best interaction between different GRID probes and COX-2 residues provided suggestions for appropriately decorating positions 1 and 3 of the pyrrole nucleus. Accordingly, the insertion of various substituents at meta and para positions of the N1 phenyl ring yielded derivatives with high affinity for (in the range of two-digit nanomolar concentrations) and selective toward (up to 10000) COX-2.[23,24,26] On the other hand, inspection of the binding mode of pyrrole derivatives bearing an acetic acid ethyl ester moiety at C3 led to the suggestion that its terminal alkyl moiety is very important for hydrophobic interactions with Val116 and Tyr355 and contributes to the strength of the complex with COX-2.[23,24,26] To further support this hypothesis, the new pyrrole derivatives **10a**−**h** were designed and synthesized, keeping fixed the SO_2Me group at the C5 phenyl ring and several substituents at the N1 phenyl ring (previously found to be key determinants of potency and COX-2 selectivity), while the size and length of the ester chain at C3 were modified by insertion of an isopropyl or butyl moiety. As expected, resulting compounds showed very strong inhibition of COX-2, with IC_{50} values ranging from 0.007 [**10a** (Table 1)] to 0.043 μM (**10c**) and a selectivity index of >2300. Docking calculations showed that the new compounds bind the COX-2 binding site with the same orientation of their previous analogues (Figure 1B). Moreover, following a trend in activity already found, ester derivatives **10a**−**h** were more active than the corresponding acid analogues (with the exception of **11c**), because of additional hydrophobic interactions between the terminal alkyl chain and residues of the carboxylate site (Leu93, Val116, Tyr355, and Leu359). GRID calculations with the C3 probe seemed to suggest that a two-carbon atom group was the optimal substituent to be inserted into the ester chain, although additional space for longer alkyl groups was available in the region where the ester alkyl chain is accommodated. Inspection of the binding mode of the new derivatives showed that both the isopropyl and the butyl chains are able to satisfy this geometrical constraint. In fact, the isopropyl moiety, having the same length of an ethyl group although larger in size, matched the GRID minimum point of the C3 probe. On the other hand, the butyl group assumed a folded conformation, leading its carbon atoms to be located around the C3 best interaction point found by GRID, and thus making similar hydrophobic contacts with enzyme residues. Moreover, both ester and acid derivatives were also able to interact by hydrogen bonds with the guanidino moiety of Arg120.

In vitro results and a SAR analysis of acids **6a** and **11c,e,g**, synthesized and tested on the basis of the hypothesis that hydrolysis of the ester moiety can occur in vivo to at least some extent, confirmed the dependence of the activity from the N1 phenyl ring substitution pattern (Table 1). Moreover, ester derivatives **10a**−**h** proved to be more active than the corresponding acids, exhibiting IC_{50} values from 4.5- to 143-fold better (compare **10a,b** vs **6a**, **10e,f** vs **11e**, and **10g,h** vs **11g**). The sole exception to this trend was represented by 3-F derivatives that exhibited comparable activity (compare **10c,d** vs **11c**). Esters also had a higher COX-1/COX-2 selectivity in comparison to the acids. Finally, all the esters **10a**−**h** were found to be more effective in inhibiting COX-2 than their ethyl analogues previously described (as an example, compare **10a** and **10b** with **6d**) (Chart 1)[23,24] or celecoxib while maintaining or even increasing COX-1/COX-2 in vitro selectivity.

In summary, analysis of the influence of substituents and substitution pattern on the activity and selectivity toward COX-2 showed that current substituents at positions N1 and C3 are optimal cooperative determinants for potent and

selective inhibitors and should be considered as structural elements for fine-tuning of affinity toward the enzyme.

Pharmacological Evaluation. Among the most interesting compounds found in the cell-based assay, **10a** and **10c**, as well as the corresponding acid derivatives, **6a** and **11c**, were selected for evaluation of the inhibitory effects toward the HWB assay for COX-1 and COX-2. Results indicated a dramatic change in terms of COX selectivity under these experimental conditions (Table 2), since celecoxib remained as selective as **6a** (selectivity indexes of 23 and 19, respectively), while the remaining compounds, **10a**, **10c**, and **11c**, showed a selectivity index of <12. The discrepancy between these results and those found in the cell-based assay could be due to a different inhibitor sensitivity exhibited by the mouse and human COX isozymes, as already reported for other anti-inflammatory compounds.[10] As a matter of the fact, such a dramatic loss in COX inhibitory potency and a drop in selectivity under the HWB assay conditions are common to other selective COX-2 inhibitors, such as valdecoxib,[31,32] etoricoxib,[31,32] lumiracoxib,[33] and rofecoxib,[34,35] as well as tNSAIDs such as nimesulide[16,31] and meloxicam.[36,37]

Table 2. Ex Vivo Inhibition (HWB) of COX-1 and COX-2 by Compounds **10a,c**, **6a**, and **11c** and Celecoxib

	IC_{50} (μM)		
compd	COX-1	COX-2	selectivity index
10a	20	2.5	8
10c	24	2	12
6a	132	7	19
11c	125	17	7
celecoxib, **1b**	12.5	0.54	23

It should be pointed out that, according to the test, **10a**, **10c**, and **11c** exhibited an affinity for COX-2 5−10-fold higher than that for COX-1, which should translate clinically into an acceptable GI safety, and allowing for a sufficient prostacyclin generation that should mitigate the CV effects showed by overly selective COX-2 inhibitors, as previously discussed.

To assess in vivo anti-inflammatory and analgesic activity of **10a**−**h**, **6a**, and **11c,e,g**, the rat paw pressure test and the paw volume and abdominal constriction tests were performed (Tables 3−5, respectively). Compounds, administered at different dosages (from 10 to 20 mg/kg po), showed a very good activity against carrageenan-induced hyperalgesia. The activity of **10a**−**h** was better than that of both the corresponding acids and ethyl esters.[23,24] Esters also proved

Table 3. Effect of Compounds **6a**, **10a**−**h**, and **11c,e,g** and Celecoxib in the Rat Paw Pressure Test

		paw pressure (g)			
pretreatment	treatment	before pretreatment	30 min after treatment	60 min after treatment	120 min after treatment
saline	saline	63.4 ± 4.6	60.2 ± 5.1	62.9 ± 4.9	60.7 ± 5.4
carrageenan	saline	61.9 ± 5.1	38.7 ± 5.3	35.8 ± 4.5	40.1 ± 5.0
carrageenan	**10a**[a]	60.8 ± 4.3	56.2 ± 4.8	51.8 ± 5.3	48.8 ± 3.7
carrageenan	**10b**[b]	57.5 ± 3.7	52.5 ± 4.9	46.3 ± 5.3	42.6 ± 3.8
carrageenan	**10c**[b]	63.2 ± 3.8	59.5 ± 5.4	57.9 ± 4.1	45.2 ± 4.3
carrageenan	**10d**[b]	62.4 ± 3.2	49.7 ± 4.1	46.9 ± 5.5	45.2 ± 4.8
carrageenan	**10e**[b]	59.5 ± 2.9	64.8 ± 3.8	52.3 ± 4.9	58.3 ± 3.4
carrageenan	**10f**[b]	58.3 ± 3.6	52.7 ± 5.0	59.2 ± 6.3	56.6 ± 4.5
carrageenan	**10g**[b]	58.6 ± 4.1	51.0 ± 5.5	56.7 ± 4.4	41.7 ± 4.1
carrageenan	**10h**[b]	60.5 ± 3.0	53.4 ± 4.8	51.4 ± 5.0	50.8 ± 5.2
carrageenan	**6a**[b]	63.1 ± 2.9	48.6 ± 4.3	51.8 ± 3.6	41.6 ± 3.7
carrageenan	**11c**[b]	62.7 ± 4.2	54.8 ± 3.7	55.2 ± 3.8	43.1 ± 3.9
carrageenan	**11e**[b]	59.2 ± 3.4	58.3 ± 3.4	54.1 ± 4.4	48.6 ± 3.4
carrageenan	**11g**[b]	61.2 ± 3.6	52.3 ± 3.7	39.8 ± 4.1	36.2 ± 3.2
carrageenan	celecoxib, **1b**[a]	62.7 ± 3.9	56.5 ± 3.8	58.2 ± 4.4	55.2 ± 5.1

[a] Compounds were administered po at a dose of 10 mg/kg. [b] Compounds were administered po at a dose of 20 mg/kg.

Table 4. Effect of Compounds **6a**, **10a**−**h**, and **11c,e,g** in Comparison to Celecoxib in the Edema Induced by Carrageenan

		paw volume (mL)		
pretreatment	treatment	before pretreatment	60 min after treatment	% of paw edema suppression
saline	saline	1.26 ± 0.09	1.31 ± 0.10	
carrageenan	saline	1.22 ± 0.08	2.33 ± 0.08	
carrageenan	**10a**[a]	1.29 ± 0.09	1.26 ± 0.12	100
carrageenan	**10b**[b]	1.31 ± 0.10	1.68 ± 0.15	66.3
carrageenan	**10c**[b]	1.17 ± 0.11	1.31 ± 0.09	87.2
carrageenan	**10d**[b]	1.35 ± 0.09	1.71 ± 0.11	67.2
carrageenan	**10e**[b]	1.29 ± 0.10	1.39 ± 0.12	89.0
carrageenan	**10f**[b]	1.23 ± 0.08	1.52 ± 0.09	73.6
carrageenan	**10g**[b]	1.16 ± 0.07	1.41 ± 0.08	77.2
carrageenan	**10h**[b]	1.33 ± 0.08	1.45 ± 0.14	89.1
carrageenan	**6a**[b]	1.23 ± 0.10	1.86 ± 0.07	42.7
carrageenan	**11c**[b]	1.28 ± 0.05	1.35 ± 0.09	93.6
carrageenan	**11e**[b]	1.32 ± 0.10	1.42 ± 0.09	90.9
carrageenan	**11g**[b]	1.27 ± 0.08	1.81 ± 0.12	50.9
carrageenan	celecoxib, **1b**[a]	1.28 ± 0.14	1.33 ± 0.10	95.5

[a] Compounds were administered po at a dose of 10 mg/kg. [b] Compounds were administered po at a dose of 20 mg/kg.

to be very effective and long-lasting, in this test a relevant analgesia being still present 2 h after administration.

Table 5. Effect of Compounds **6a**, **10a**−**h**, and **11c,e,g** in Comparison to Celecoxib in the Mouse Abdominal Constriction Test (0.6% acetic acid)

treatment[a]	no. of mice	dose (mg/kg po)	no. or writhes
CMC[b]	20		31.4 ± 4.3
10a	8	1	33.6 ± 3.0
10a	8	5	28.5 ± 3.3[c]
10a	8	15	25.5 ± 2.8[c]
10b	8	20	23.9 ± 3.4[c]
10c	12	5	39.5 ± 3.8
10c	9	20	17.7 ± 2.9[c]
10d	8	20	24.4 ± 4.1[c]
10e	10	5	35.1 ± 4.6
10e	12	20	21.5 ± 3.9[c]
10e	10	40	19.8 ± 3.2[c]
10f	12	5	34.4 ± 3.5
10f	30	20	13.7 ± 4.0[c]
10g	11	5	42.2 ± 4.0
10g	12	20	18.0 ± 3.5[c]
10h	8	10	21.6 ± 2.9[c]
10h	10	20	15.9 ± 3.3[c]
6a	11	10	27.3 ± 3.2
11a	10	20	22.2 ± 2.9
11c	9	10	31.6 ± 3.2
11c	8	20	17.5 ± 3.1
11e	12	10	29.3 ± 3.0
11e	10	20	15.7 ± 2.6
11g	10	10	30.9 ± 3.3
11g	10	20	21.8 ± 2.1
celecoxib, **1b**	12	10	14.2 ± 2.3

[a] All the compounds were administered po 30 min before the test. [b] CMC is carboxymethylcellulose. [c] $p < 0.01$ vs vehicle-treated mice.

Table 6. Metabolic Stability of Compounds **6a**, **10a**−**h**, and **11c,e,g**

compd	mean parent remaining (%) (test concentration, 10 μM)	mean parent remaining (%) (test concentration, 0.1 μM)
6a	97	94
11c	100	100
11e	100	100
11g	84	77
10a	1	11
10b	3	7
10c	1	0
10d	2	0
10e	13	0
10f	15	2
10g	1	7
10h	2	5

Table 7. Analgesic Activity of **10a** and Celecoxib in the Randall−Selitto Model of Zymosan-Induced Hyperalgesia in Rats

compd	analgesia for 0−2 h MPE (%)	analgesia for 0−6 h MPE (%)
10a	75	70
celecoxib, **1b**	30	35

The most active compounds were **10e**, **10f**, and **10h** (Table 3). Conversely, the corresponding acids **6a** and **11c, e,g** had a remarkably lower activity (especially after 2 h), except for **11e** whose activity was comparable to that of **10a**. Moreover, a very good activity was found toward carrageenan-induced edema in the rat paw (Table 4), with a complete remission 1 h after administration (20 mg/kg po). Among the test compounds, **10a**, **10c**, and **11c** showed the best activity. Finally, a dose-dependent antinociceptive activity was also observed in the abdominal constriction test (Table 5), **10f**, **10h**, **11c**, and **11e** exhibiting remarkable activity.

The metabolic stability of the compounds was also evaluated using human liver microsomes (Table 6). Acids **6a** and **11c,e** had high stability, thus indicating that the 1,5-diarylpyrrole scaffold is not liable to metabolic attack, even with an unsubstituted N1 phenyl ring as in **6a**. The lower stability of **11g** suggests that the 4-methoxy group can give rise to some metabolic liability. Conversely, esters **10a**−**h** were liable to hepatic metabolism at concentrations of both 10^{-5} and 10^{-7} M, thus suggesting hydrolysis at the ester moiety as the major metabolic pathway for these compounds, even when hindered esters (such as isopropyl) are taken into account.

Compound **10a** was then selected for further studies, because of the low activity of its acid analogue **6a**. This choice was made to avoid issues caused by a possible in vivo metabolism to an overly active metabolite, as in the case of **11c** and **11e**. Compound **10a** was evaluated in comparison to celecoxib in the Randall−Selitto model of zymosan-induced hyperalgesia[38] in rats. Compounds were administered orally as a 0.5% suspension in methocel at doses of 1, 3, and 5 mg/kg. Table 7 reports results of a 3 mg/kg dose administration, expressed as the maximum percentage effect (MPE). In this model, ED_{50} values for **10a** and celecoxib were 2.2 and 9.0 mg/kg, respectively. Accordingly, **10a** was more potent than celecoxib and was endowed with a longer duration of action. To exclude the possibility that these results were due to any impairment effect, **10a** was finally evaluated in the rota-rod test. Mice treated with test compound at a dose of 25 mg/kg po did not exhibit a larger number of falls from the rotating rod in comparison with controls (Table 8). Therefore, **10a** did not cause any alteration in mouse motor coordination.

Pharmacokinetic Study. The pharmacokinetics of **10a** was assessed in rats after po and iv administration of the compound. Profiles of the plasma concentration versus time after po and iv administration of **10a** (10 mg/kg) are reported in Figure 2. Compound **10a** was sufficiently absorbed, its absolute bioavailability being 42% (F%). The clearance after iv treatment (~2 L/h) was higher than the rate of blood flow in the rat (0.8 L/h),[32] thus indicating that **10a** is a high-clearance drug. The volume of distribution after iv treatment (~5.6 L) was higher than the total volume of body fluid in the rat (0.17 L),[32] indicating extensive distribution of **10a** into extravascular compartments. When compared to the clearance data, this result could explain the steady state observed in the plasma concentration for up to 5 h. The calculated

Table 8. Lack of an Effect of **10a** on Mice in the Rota-Rod Test[a]

treatment	dose (mg/kg po)	before treatment	15 min after treatment	30 min after treatment	45 min after treatment	60 min after treatment
CMC		4.2 ± 0.4	2.9 ± 0.3	1.7 ± 0.4	0.9 ± 0.2	0.7 ± 0.2
10a	25	4.2 ± 0.5	2.8 ± 0.4	2.7 ± 0.5	1.1 ± 0.3	0.8 ± 0.2

[a] Each value represents the mean of values from eight mice. The test was performed 30 min after treatment.

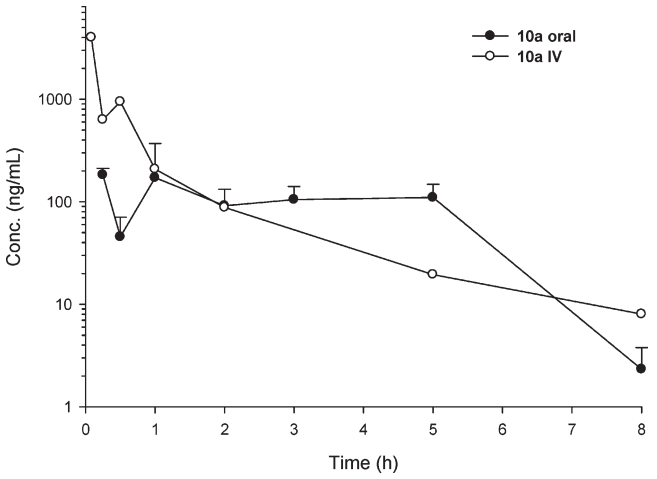

Figure 2. Profile of plasma concentration vs time after iv and po administration of **10a** (10 mg/kg).

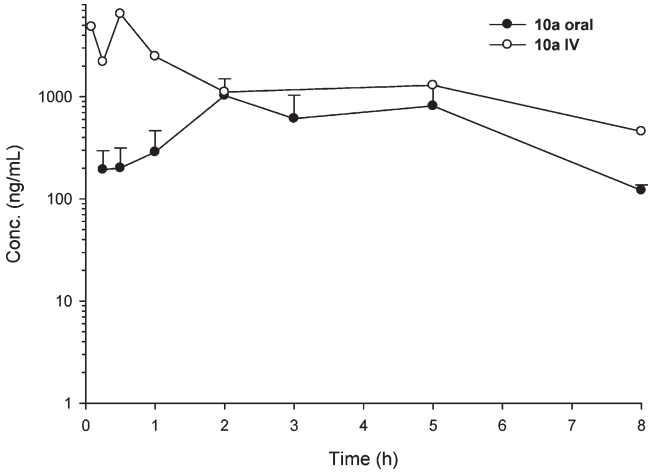

Figure 3. Concentrations (nanograms per milliliter) of **6a** vs time after iv and po administration of **10a** (10 mg/kg).

concentration of the drug within the 1−5 h time frame indicates a concentration of at least 240 nM, significantly higher than the COX-2 IC_{50} of **10a**. These pharmacokinetic data fit well with the observed long-lasting pharmacological activity in the rat. In addition, the plasmatic levels of the expected metabolite **6a** were evaluated to gain additional information about impacts exerted by this possible metabolic pathway on the overall pharmacological profile. Profiles of the plasma concentration versus time for **6a** after iv and po administration of **10a** (10 mg/kg) are reported in Figure 3. After both oral and iv administration of **10a**, the formation of **6a** was observed, thus confirming hydrolysis of the ester to the corresponding acid. The fact that the concentration of **6a** reached the same level in a manner independent of the administration route of **10a** suggested that **10a** was not largely hydrolyzed in the GI tract during the absorption but rather was formed by either plasmatic or hepatic metabolism due to esterase activity. Plasmatic concentrations versus time of **10a** and **6a** are compared in Figure 4. The circulating concentration of acid **6a** is 1 order of magnitude higher than that of ester **10a**, within the 2−5 h time frame. However, since the difference of the in vitro potency between **10a** and **6a** is 3 orders of magnitude, in vivo activity observed during the first 5 h should mostly depend

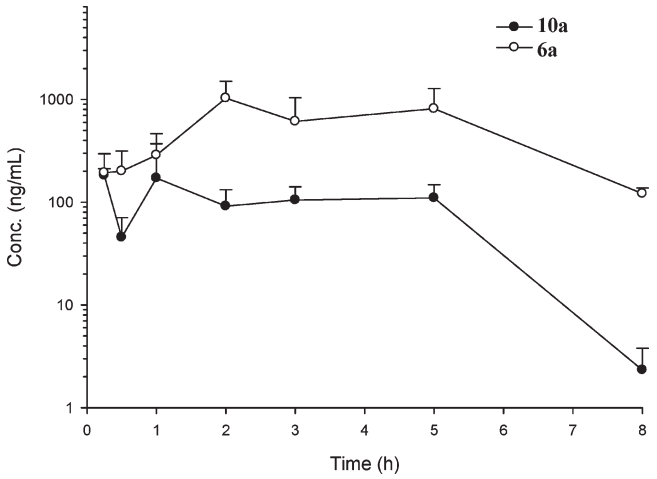

Figure 4. Plasmatic concentrations vs time of **10a** compared to the corresponding plasmatic concentrations of **6a** after oral administration of **10a** (10 mg/kg).

on the presence of ester **10a**, assuming a similar protein binding for both **10a** and **6a**. Beginning 6 h after administration, the contribution of acid **6a** to the residual activity could become relevant.

Conclusions

On the basis of previously published data and suggestions derived from both SAR analysis and molecular modeling simulations on 1,5-diarylpyrrole derivatives, a new series of compounds has been designed and synthesized. Biological data showed a significant enhancement of their biological activity with respect to the parent compounds. One of the new entries (namely, **10a**) was selected for pharmacokinetic and pharmacodynamic studies. It was approximately 8-fold more potent toward COX-2 than COX-1 in the HWB assay, and it was characterized by a high volume of distribution, suggesting its accumulation in target sites which may explain its long-lasting pharmacological activity. This pharmacokinetic feature (i.e., high volume of distribution) might translate into fast clearance from side effect compartments (including vascular wall, heart, and kidney).[31] This possibility will be explored in further studies.

The remarkable activity of these new compounds, as well as their pharmacokinetic profile, is meaningful for the development of new compounds that could be effective and safe agents for the pharmacological management of inflammation and pain.

Experimental Section

Chemistry. A Discovery Microwave System apparatus (from CEM) was used for the Stetter and Paal−Knorr reactions. All chemicals used were of reagent grade. Yields refer to purified products and are not optimized. Melting points were determined in open capillaries on a Gallenkamp apparatus and are uncorrected. Microanalyses were conducted on a Perkin-Elmer 240C or a Perkin-Elmer Series II CHNS/O Analyzer 2400 instrument. Fluka silica gel 60 (230−400 mesh) was used for column chromatography. Fluka TLC plates (silica gel 60 F254) were used for thin-layer chromatography (TLC). Fluka aluminum oxide (activity II−III, according to Brockmann) was used for chromatographic purifications. Fluka Stratocrom aluminum oxide plates with a fluorescent indicator were used for TLC to check the purity of the compounds. ^{13}C NMR and ^{1}H NMR spectra were recorded with a Bruker AC 400 spectrometer in the

indicated solvent (TMS as the internal standard). The values of the chemical shifts are expressed in parts per million and the coupling constants (*J*) in hertz.

HPLC Analysis. Analyses were conducted using a Waters Alliance 2695 instrument, using a UV−vis Waters PDA 996 detector and working at 333 nm. Millennium Empower with Windows XP was used. A Phenomenex LUNA C8, 5 μm (150 mm × 4.6 mm) column (code 00F-4249-E0), at 40 °C, was used as the chromatographic column at a flow rate of 1.0 mL/min. The eluant was (A) a 65/15/20 (v/v/v) 10 mM (pH 2.5) KH_2PO_4/MeOH/acetonitrile mixture or (B) a 15/75/10 (v/v/v) 10 mM (pH 2.5) KH_2PO_4/MeOH/acetonitrile mixture. A gradient from 100% A to 100% B was run in 25 min, and then isocratic conditions at 100% B were maintained for an additional 10 min. Using the analytical conditions reported above, the retention times of the compounds are 19.8 min. All the synthesized compounds were ≥95% pure.

1-[4-(Methylthio)phenyl]pentane-1,4-dione (12). A solution of 4-methylthiobenzaldehyde (11.97 mL, 0.09 mol), triethylamine (19.5 mL, 0.14 mol), methyl vinyl ketone (5.8 mL, 0.09 mol), and 3-ethyl-5-(2-hydroxyethyl)-4-methylthiazolium bromide (3.53 g, 0.014 mol) was put into a round-bottom flask equipped with a stir bar. The flask was inserted into the cavity of the microwave system apparatus and heated (150 W for 15 min, internal temperature of 70 °C, internal pressure of 60 psi).[28] The residue was treated with 2 N HCl (10 mL). After extraction with ethyl acetate, the organic layer was washed with aqueous sodium bicarbonate and water. The organic fractions were dried over Na_2SO_4, filtered, and concentrated to give a crude orange liquid. After crystallization from cyclohexane, intermediate **12** was isolated as white needles (78% yield). Analytical data, the melting point, and the ^{1}H NMR spectrum were consistent with those reported in the literature.[23−26]

1-[4-(Methylsulfonyl)phenyl]pentane-1,4-dione (13). To a solution of **12** (7.8 g, 35 mmol) in methanol (150 mL) was added Oxone (37.7 g, 61.4 mmol), dissolved in water (150 mL), over 5 min. After being stirred at 25 °C for 2 h, the reaction mixture was diluted with water (400 mL) and extracted with dichloromethane. The organic layer was washed with brine (200 mL) and water (200 mL) and dried (Na_2SO_4). After filtration and concentration, the crude material was chromatographed (silica gel, 3:1 hexane/ethyl acetate) to give **13** (90% yield) as a white solid. Analytical data, the melting point, and the ^{1}H NMR spectrum were consistent with those reported in the literature.[23−26]

General Procedure for the Preparation of 1,5-Diarylpyrroles 14a,c,e,g. Following the Paal−Knorr reaction, **13** (0.58 g, 2.28 mmol) was dissolved in ethanol (2 mL) in a round-bottom flask equipped with a stir bar. The suitable amine (2.28 mmol) and *p*-toluenesulfonic acid (30 mg, 0.17 mmol) were added. The flask was inserted into the cavity of the microwave system apparatus and heated (150 W for 45 min, internal temperature of 160 °C, internal pressure of 150 psi).[28] The reaction mixture was cooled and concentrated. The crude material was purified by chromatography on aluminum oxide with a 3:1 cyclohexane/ethyl acetate mixture, as the eluant, to give the expected 1,5-diarylpyrroles **14a,c,e,g** as solids in satisfactory yield.

2-Methyl-5-[4-(methylsulfonyl)phenyl]-1-phenyl-1*H*-pyrrole (14a). White needles (80% yield). Analytical data, the melting point, and the ^{1}H NMR spectrum were consistent with those reported in the literature.[29]

General Procedure for the Preparation of 1,5-Diarylpyrrol-3-glyoxylic Esters 15a−h. To a solution of the appropriate pyrrole [**14a**, **14c**, **14e**, or **14g** (4.82 mmol)] in anhydrous dichloromethane, under a nitrogen flow, were added 2,6-lutidine (0.56 mL, 4.82 mmol) and oxalyl chloride (0.40 mL, 4.82 mmol) at 0 °C. The solution was stirred for 4 h at room temperature, and then the suitable alcohol (4.82 mmol) was added. The mixture was then washed with water and extracted with $CHCl_3$. The organic solution was washed with a saturated aqueous NaCl solution, dried, and evaporated in vacuo. Purification of the residue by flash chromatography with ethyl acetate as the eluant gave a solid which, after recrystallization from hexane, afforded the expected products **15a−h**.

Isopropyl-2-methyl-5-[4-(methylsulfonyl)phenyl]-1-phenyl-1*H*-pyrrole-3-glyoxylate (15a): yellowish needles (76% yield); mp 60 °C; ^{1}H NMR ($CDCl_3$) δ 7.74−7.78 (m, 2H), 7.23−7.26 (m, 3H), 7.04−7.05 (m, 3H), 5.26 (m, 1H), 2.94−3.00 (s, 3H), 2.42- 2.46 (s, 3H), 1.33−1.41 (d, 6H).

General Procedure for the Preparation of 1,5-Diarylpyrrole-3-acetic Esters 10a−h. To a solution of the suitable α-keto ester [**15a−h** (2.3 mmol)] in TFA (9 mL, 0.12 mol) stirred at 0 °C under a nitrogen flow was slowly added triethylsilane (0.75 mL, 4.7 mmol), and the mixture was stirred for 2 h at room temperature. At the end of the reaction, the mixture was made alkaline with 40% aqueous ammonia (10 mL) and extracted with $CHCl_3$. The organic solution was dried and evaporated in vacuo. The resulting residue was chromatographed on silica gel eluting with $CHCl_3$ to give a solid which, after recrystallization from hexane, afforded the desired products **10a−h**.

Isopropyl-2-methyl-5-[4-(methylsulfonyl)phenyl]-1-phenyl-1*H*-pyrrole-3-acetate (10a). Yellowish needles (yield 55%). Analytical data, the melting point, and the ^{1}H NMR spectrum were consistent with those reported in the literature:[27] ^{13}C NMR δ 11.00 (CH_3 pyrrolic), 21.82 (CH_3 isopropyl), 32.62 (CH_2), 44.41 (CH_3 sulfonyl), 68.03 (CH isopropyl), 112.58 (CH pyrrole), 114.04 (C_q pyrrole), 127.12, 127.30, 128.10, 128.40, 129.40 (CH aromatic), 131.10, 131.60, 136.55, 138.50, 138.92 (C_q aromatic), 171.67 (COO).

General Procedure for the Preparation of Ethyl 1,5-Diarylpyrrol-3-ylglyoxylic Esters 16a,c,e,g. To a solution of the appropriate pyrrole [**14a**, **14c**, **14e**, or **14g** (4.82 mmol)] in anhydrous dichloromethane, under a nitrogen flow, were added $TiCl_4$ (0.53 mL, 4.82 mmol) and etoxalyl chloride (0.54 mL, 4.82 mmol) at 0 °C. The solution was stirred for 4 h at room temperature. The mixture was then washed with water and extracted with $CHCl_3$. The organic solution was washed with a saturated aqueous NaCl solution, dried, and evaporated in vacuo. Purification of the residue by flash chromatography with $CHCl_3$ as the eluant gave a solid which, after recrystallization from hexane, afforded the expected products **16a,c,e,g**.

Ethyl-2-methyl-5-[4-(methylsulfonyl)phenyl]-1-phenyl-1*H*-pyrrole-3-glyoxylate (16a). White needles (76% yield). Analytical data, the melting point, and the ^{1}H NMR spectrum were consistent with those reported in the literature.[25]

General Procedure for the Preparation of Ethyl 1,5-Diarylpyrrole-3-acetic Esters 17a,c,e,g. Compounds **17a,c,e,g** were obtained from **16a,c,e,g**, respectively, according to the procedure described for **10a−h**.

Ethyl-2-methyl-5-[4-(methylsulfonyl)phenyl]-1-phenyl-1*H*-pyrrole-3-acetate (17a). White solid (68% yield). Analytical data, the melting point, and the ^{1}H NMR spectrum were consistent with those reported in the literature.[25]

General Procedure for the Preparation of 1,5-Diarylpyrrole-3-acetic Acids 6a and 11c,e,g. To a solution of the appropriate ethyl 1,5-diarylpyrrole-3-acetic esters **17a,c,e,g** (0.30 g, 0.67 mmol) in methanol (4.83 mL) was added 4.83 mL of 1 N NaOH. The resulting mixture was refluxed for 1 h, cooled, and concentrated in vacuo. The residue was solubilized in water and then acidified with concentrated HCl. The precipitate was filtered to give the desired acids **6a** and **11c,e,g** as white solids.

2-Methyl-5-[4-(methylsulfonyl)phenyl]-1-phenyl-1*H*-pyrrol-3-acetic Acid (6a). White solid (71% yield). Analytical data, the melting point, and the ^{1}HNMR spectrum were consistent with those reported in the literature:[23] ^{13}C NMR δ 11.10 (CH_3 pyrrolic), 32.90 (CH_2), 44.41 (CH_3 sulfonyl), 112.60 (CH pyrrole), 114.05 (C_q pyrrole), 127.14, 127.32, 128.15, 128.42, 129.44 (CH aromatic), 131.15, 131.66, 136.55, 138.50, 138.98 (C_q aromatic), 177.67 (COO).

Biology. In Vitro Anti-Inflammatory Study. Compounds **10a−h**, **6a**, and **11c,e,g** were all evaluated for their inhibitory activity toward both COX-2 and COX-1 enzymes.

The murine monocyte/macrophage J774 cell line was grown in DMEM supplemented with 2 mM glutamine, 25 mM HEPES, 100 units/mL penicillin, 100 μg/mL streptomycin, 10% fetal bovine serum (FBS), and 1.2% sodium pyruvate. Cells were plated in 24-well culture plates at a density of 2.5×10^5 cells/mL or in 60 mm diameter culture dishes (3×10^6 cells per 3 mL per dish) and allowed to adhere at 37 °C in 5% CO_2 for 2 h.

Immediately before the experiments, culture medium was replaced with fresh medium without FBS and cells were stimulated as described previously.[39]

To evaluate COX-1 activity, cells were pretreated with test compounds (0.01−10 μM) for 15 min and further incubated at 37 °C for 30 min with 15 μM arachidonic acid to activate the constitutive COX. At the end of the incubation, the supernatants were collected for the measurement of prostaglandin E_2 (PGE_2) levels by a radioimmunoassay (RIA). On the other hand, to evaluate COX-2 activity, cells were stimulated for 24 h with *Escherichia coli* lipopolysaccharide (LPS, 10 μg/mL) to induce COX-2, in the absence or presence of test compounds, at the concentrations previously reported. Celecoxib was utilized as a reference compound for the selectivity index. The supernatants were collected for the measurement of PGE_2 by RIA. Throughout the time the experiments lasted, triplicate wells were used for the various conditions of treatment. Results are expressed as the mean, for three experiments, of the percent inhibition of PGE_2 production by test compounds with respect to control samples. The IC_{50} values were calculated with GraphPad Instat, and the data fit was obtained using the sigmoidal dose−response equation (variable slope) (GraphPad).

Ex Vivo Anti-Inflammatory Study. Compounds **10a−h**, **6a**, and **11c,e,g** were also evaluated for COX-1 versus COX-2 selectivity by means of the HWB assay. To evaluate COX-2 activity, 1 mL aliquots of peripheral venous blood samples were incubated in the presence of LPS (10 μg/mL) or saline for 24 h at 37 °C as previously described.[18] As an index of LPS-induced monocyte COX-2 activity, PGE_2 plasma levels were measured by RIA.[18] A COX-1 assay was performed on peripheral venous blood samples drawn from the same donors when they had not taken any NSAID during the 2 weeks preceding the study. Whole blood thromboxane B_2 production was measured by RIA, as a reflection of maximally stimulated platelet COX-1 activity in response to endogenously formed thrombin.[31] Celecoxib was tested at final concentrations of 0.01−100 μM in both COX-2 and COX-1 assay.

In Vivo Anti-Inflammatory Study. In vivo anti-inflammatory activity of the new compounds was also assessed. Male Swiss albino mice (23−25 g) and Sprague-Dawley or Wistar rats (150−200 g) were used. The animals were fed with a standard laboratory diet and tap water ad libitum and kept at 23 ± 1 °C with a 12 h light/dark cycle, light on at 7 a.m. The paw pressure test was performed by inducing an inflammatory process in the administered ip carrageenan 4 h before the test. The carrageenan-induced paw edema test was also performed, evaluating the paw volume of the right hind paw 5 h after the injection of carrageenan and comparing it with saline/carrageenan-treated controls. The analgesic activity of compounds was also assessed by performing the abdominal constriction test, using mice into which a 0.6% solution of acetic acid (10 mL/kg) had been injected ip. The number of stretching movements was counted for 10 min, starting 5 min after administration.

The rota-rod test was performed as previously described.[40] Potential motor incoordination/ataxia caused by compound injection was evaluated using a rota-rod apparatus in which animals were required to walk against the motion of a rotating drum for 30 s. The time taken to fall off the rota-rod was recorded as the number of falls in 30 s. The rod (30 cm long) was divided into five equal section by six disks. Thus, up to five mice were tested simultaneously on the apparatus, with a rod rotation of 16 rpm.

Zymosan-Induced Hyperalgesia. The interplantar injection of zymosan-induced mechanical hyperalgesia is a model of inflammatory pain.[38] In this model, a male Sprague-Dawely or Wistar rat (200−250 g) receives an interplantar injection of 4 mg of zymosan/100 μL into one hind paw; a marked inflammation occurs. Compounds were administered orally for evaluation of efficacy, 30 min before the inflammatory insult. The hyperalgesia induced by zymosan administration was evaluated using the Randal−Selitto method.[41] The quantitation of the analgesic effect was achieved by an analgesimeter, which consists of application to the inflamed paw an increasing weight (from 130−140 to 500 g). The difference in the mechanical pain threshold between the basal value (generally, 230−250 g) and the one tolerated by the animals treated with the drug, determined 4 h after the inflammatory challenge, is defined as mechanical hyperalgesia. Mechanical hyperalgesia is expressed as the maximum percent effect (MPE) that represents the difference (percent) in pain threshold between the animals treated with the drug and the controls that received only the vehicle. Results are reported as MPE (reduction of the nociceptive effect, due to paw loading with increasing weight, in comparison to controls); 100% MPE means that the animal treated with the compound and zymosan can tolerate the same stimulus (weight) as the control animals which have not received zymosan treatment. An MPE higher than 100% means that the animal treated with the compound and zymosan can tolerate stimuli (weight) more than the control animals, which has not received zymosan treatment (hypoalgesia).

In Vitro Metabolic Stability in Human Liver Microsomes. Metabolic stability was evaluated on human liver microsomes incubated for 60 min at 37 °C with test compounds (0.1 and 10 μM), NADP (1 mM), D-glucose 6-phosphate (G6P) (6 mM), glucose-6-phosphate dehydrogenase (G6PDHase) (1 unit/mL), 0.6% methanol, 0.6% acetonitrile ($n = 2$), and phosphate buffer (pH 7.4). At the end of the incubation at each of the time points, an equal volume of an organic mixture [50:50 (v/v) acetonitrile/methanol] was added to the incubation mixture followed by centrifugation. Peak areas corresponding to the analytes were determined by HPLC−MS/MS. The ratio of the precursor compound remaining at the end of the incubation to the amount remaining at time zero, expressed as a percent value, is reported as metabolic stability.

Pharmacokinetic Study. Male Sprague-Dawley rats, three animals per time point, were treated with each compound (10 mg/kg), dissolved in DMSO either po or iv. Approximately 0.3 mL of blood per time point was taken from the retro-orbital sinus using a capillary tube. Blood samples were collected into sodium heparin-labeled tubes and treated with NaF to minimize ester hydrolysis. The samples where then centrifugated at 2500 rpm for 5 min at 4 °C. Plasma was separated, placed in prelabeled Eppendorf tubes, and stored at −20 °C pending the assay. The samples were analyzed by HPLC with UV detection, and the LOQ was 1.0 ng/mL. Pharmacokinetic calculations were performed using the kinetic software by noncompartmental methods.

Computational Details. Calculations were performed according to a computational protocol previously described.[23,24] Figure 1 has been generated by means of AutoDockTools version 1.5.1. The MSMS (maximal speed molecular surface) module of AutoDock has been used to graphically represent a section of the enzyme molecular surface. In particular, a clipping plan parallel to the ligand pyrrole ring has been applied to the protein molecular surface to show regions of the binding site accessible to ligands.

Acknowledgment. We thank Rottapharm SpA (Monza, Italy) for financial support of this research. The HWB assay was supported by a grant from MIUR to P.P.

Supporting Information Available: Physicochemical, spectroscopical, and analytical data of compounds. This material is available free of charge via the Internet at http://pubs.acs.org.

References

(1) Burke, A.; Smyth, E.; FitzGerald, G. A. Autacoids: Drug Therapy of Inflammation. In *The Pharmacological Basis of Therapeutics*, 11th ed.; Brunton, L. L., Lazo, J. S., Parker, K. L., Eds.; Macmillan Publishing Co.: New York, 2005; pp 671−736.

(2) FitzGerald, G. A.; Patrono, C. The coxibs, selective inhibitors of cyclooxygenase-2. *N. Engl. J. Med.* **2001**, *345*, 433–442.

(3) Bombardier, C.; Laine, L.; Reicin, A.; Shapiro, D.; Burgos-Vergas, R.; Davis, B.; Day, R.; Ferraz, M. B.; Hawkey, C. J.; Hochberg, M. C.; Kvien, T. K.; Schnitzer, T. J. Comparison of upper gastrointestinal toxicity of rofecoxib and naproxen in patients with rheumatoid arthritis. VIGOR study group. *N. Engl. J. Med.* **2000**, *343*, 1520–1528.

(4) Schnitzer, T. J.; Burmester, G. R.; Mysler, E.; Hochberg, M. C.; Doherty, M.; Ehrsam, E.; Gitton, X.; Krammer, G.; Mellein, B.; Matchaba, P.; Gimona, A.; Hawkey, C. J. Comparison of lumiracoxib with naproxen and ibuprofen in the Therapeutic Arthritis Research and Gastrointestinal Event Trial (TARGET), reduction in ulcer complications: Randomised controlled trial. *Lancet* **2004**, *364*, 676–684.

(5) Fries, S.; Grosser, T.; Price, T. S.; Lawson, J. A.; Kapoor, S.; DeMarco, S.; Pletcher, M. T.; Wiltshire, T.; FitzGerald, G. A. Marked interindividual variability in the response to selective inhibitors of cyclooxygenase-2. *Gastroenterology* **2006**, *130*, 55–64.

(6) Grosser, T.; Fries, S.; FitzGerald, G. A. Biological basis for the cardiovascular consequences of COX-2 inhibition: Therapeutic challenges and opportunities. *J. Clin. Invest.* **2006**, *116*, 4–15.

(7) http://www.emea.europa.eu/pdfs/human/press/pr/PR_Lumiracoxib_57930107en.pdf, accessed October 29, **2009**.

(8) Capone, M. L.; Tacconelli, S.; Di Francesco, L.; Sacchetti, A.; Sciulli, M. G.; Patrignani, P. Pharmacodynamic of cyclooxygenase inhibitors in humans. *Prostaglandins Other Lipid Mediators* **2007**, *82*, 85–94.

(9) Ferdinandi, E. S.; Cayen, M. N.; Pace-Asciak, C. Disposition of etodolac, other anti-inflammatory pyranoindole-1-acetic acids and furobufen in normal and adjuvant arthritic rats. *J. Pharmacol. Exp. Ther.* **1982**, *220*, 417–426.

(10) Engelhardt, G.; Homma, D.; Schlegel, K.; Utzmann, R.; Schnitzler, C. Anti-inflammatory, analgesic, antipyretic and related properties of meloxicam, a new non-steroidal anti-inflammatory agent with favourable gastrointestinal tolerance. *Inflammation Res.* **1995**, *44*, 423–433.

(11) Weissenbach, R. Clinical trial with Nimesulide, a new non-steroid anti-inflammatory agent, in rheumatic pathology. *J. Int. Med. Res.* **1981**, *9*, 349–352.

(12) Ku, E. C.; Wasvary, J. M.; Cash, W. D. Diclofenac sodium (GP 45840, Voltaren), a potent inhibitor of prostaglandin synthetase. *Biochem. Pharmacol.* **1975**, *24*, 641–643.

(13) Prasit, P.; Wang, Z.; Brideau, C.; Chan, C. C.; Charleson, S.; Cromlish, W.; Ethier, D.; Evans, J. F.; Ford-Hutchinson, A. W.; Gauthier, J. Y.; Gordon, R.; Guay, J.; Gresser, M.; Kargman, S.; Kennedy, B.; Leblanc, Y.; Leger, S.; Mancini, J.; O'Neill, G. P.; Quellet, M.; Percival, M. D.; Perrier, H.; Riendeau, D.; Rodger, I.; Tagari, P.; Therien, M.; Vickers, P.; Wong, E.; Xu, L. J.; Young, R. N.; Zamboni, R.; Boyce, S.; Rupniak, N.; Forrest, M.; Visco, D.; Patrick, D. The discovery of rofecoxib, [MK 966, Vioxx, 4-(4′-methylsulfonylphenyl)-3-phenyl-2(5*H*)-furanone], an orally active cyclooxygenase-2-inhibitor. *Bioorg. Med. Chem. Lett.* **1999**, *9*, 1773–1778.

(14) Penning, T. D.; Talley, J. J.; Bertenshaw, S. R.; Carter, J. S.; Collins, P. W.; Docter, S.; Graneto, M. J.; Lee, L. F.; Malecha, J. W.; Miyashiro, J. M.; Rogers, R. S.; Rogier, D. J.; Yu, S. S.; Anderson, G. D.; Burton, E. G.; Cogburn, J. N.; Gregory, S. A.; Koboldt, C. M.; Perkins, W. E.; Seibert, K.; Veenhuizen, A. W.; Zhang, Y. Y.; Isakson, P. C. Synthesis and biological evaluation of the 1,5-diarylpyrazole class of cyclooxygenase-2 inhibitors: Identification of 4-[5-(4-methylphenyl)-3-(trifluoromethyl)-1*H*-pyrazol-1-yl]benzenesulfonamide (SC-58635, celecoxib). *J. Med. Chem.* **1997**, *40*, 1347–1365.

(15) Talley, J. A.; Brown, D. L.; Carter, J. S.; Masferrer, M. J.; Perkins, W. E.; Rogers, R. S.; Shaffer, A. F.; Zhang, Y. Y.; Zweifel, B. S.; Seiberk, K. 4-[5-Methyl-3-phenylisoxazol-4-yl]benzenesulfonamide, valdecoxib: A potent and selective inhibitor of COX-2. *J. Med. Chem.* **2000**, *43*, 775–777.

(16) Riendeau, D.; Percival, M. D.; Brideau, C.; Charleson, S.; Dube, D.; Ethier, D.; Falgueyret, J.-P.; Friesen, R. W.; Gordon, R.; Greig, G.; Guay, I.; Manacini, J.; Ouellet, M.; Wong, E.; Xu, L.; Boyce, S.; Visco, D.; Girad, Y.; Prasit, P.; Zamboni, R.; Rodger, J. W.; Gresser, M.; Ford-Hutchinson, A. W.; Young, R. N.; Chan, C.-C. Etoricoxib (MK-0663): Preclinical profile and comparison with other agents that selectively inhibit cyclooxygenase-2. *J. Pharmacol. Exp. Ther.* **2001**, *296*, 558–566.

(17) Ding, C.; Jones, G. Lumiracoxib (Novartis). *IDrugs* **2002**, *5*, 1168–1172.

(18) Patrignani, P.; Panara, M. R.; Greco, A.; Fusco, O.; Natoli, C.; Iacobelli, S.; Cipollone, F.; Ganci, A.; Crèminon, C.; Maclouf, J.; Patrono, C. Biochemical and pharmacological characterization of the cyclooxygenase activity of human blood prostaglandin endoperoxide synthases. *J. Pharmacol. Exp. Ther.* **1994**, *271*, 1705–1712.

(19) Patrignani, P.; Panara, M. R.; Sciulli, M. G.; Santini, G.; Renda, G.; Patrono, C. Differential inhibition of human prostaglandin endoperoxide synthase-1 and -2 by nonsteroidal anti-inflammatory drugs. *J. Physiol. Pharmacol.* **1997**, *48*, 623–631.

(20) Huntjens, D. R.; Danhof, M.; Della Pasqua, O. E. Pharmacokinetic-pharmacodynamic correlations and biomarkers in the development of COX-2 inhibitors. *Rheumatology* (*Oxford, U.K.*) **2005**, *44*, 846–859.

(21) Hernandez-Diaz, S.; Varas-Lorenzo, C.; Garcia Rodriguez, L. A. Non-steroidal antiinflammatory drugs and the risk of acute myocardial infarction. *Basic Clin. Pharmacol. Toxicol.* **2006**, *98*, 266–274.

(22) Kearney, P. M.; Baigent, C.; Godwin, J.; Halls, H.; Emberson, J. R.; Patrono, C. Do selective cyclo-oxygenase-2 inhibitors and traditional non-steroidal anti-inflammatory drugs increase the risk of atherothrombosis? Meta-analysis of randomised trials. *Br. Med. J.* **2006**, *332*, 1302–1305.

(23) Biava, M.; Porretta, G. C.; Cappelli, A.; Vomero, S.; Botta, M.; Manetti, F.; Giorgi, G.; Sautebin, L.; Rossi, A.; Makovec, F.; Anzini, M. 1,5-Diarylpyrrole-3-acetic acids and esters as novel classes of potent and selective COX-2 inhibitors. *J. Med. Chem.* **2005**, *48*, 3428–3432.

(24) Biava, M.; Porretta, G. C.; Poce, G.; Supino, S.; Cappelli, A.; Vomero, S.; Manetti, F.; Botta, M.; Sautebin, L.; Rossi, A.; Ghelardini, C.; Vivoli, E.; Makovec, F.; Anzellotti, P.; Patrignani, P.; Anzini, M. COX-2 inhibitors. 1,5-Diarylpyrrole-3-acetic esters with enhanced inhibitory activity toward COX-2 and improved COX-2/COX-1 selectivity. *J. Med. Chem.* **2007**, *50*, 5403–5411.

(25) Anzini, M.; Rovini, M.; Cappelli, A.; Vomero, S.; Manetti, F.; Botta, M.; Sautebin, L.; Rossi, A.; Ghelardini, C.; Norcini, M.; Giordani, A.; Makovec, F.; Anzellotti, P.; Patrignani, P.; Biava, M. Synthesis, biological evaluation, and enzyme docking simulations of 1,5-diarylpyrrole-3-alkoxyethyl ethers as highly selective COX-2 inhibitors endowed with anti-inflammatory and antinociceptive activity. *J. Med. Chem.* **2008**, *51*, 4476–4481.

(26) Biava, M.; Porretta, G. C.; Poce, G.; Supino, S.; Manetti, F.; Botta, M.; Sautebin, L.; Rossi, A.; Pergola, C.; Ghelardini, C.; Norcini, M.; Makovec, F.; Anzellotti, P.; Cirilli, R.; Ferretti, R.; Gallinella, B.; La Torre, F.; Anzini, M.; Patrignani, P. Chiral alcohol and et her derivatives of the 1,5-diarylpyrrole scaffold as novel antiinflammatory and analgesic agents. Synthesis, in vitro and in vivo biological evaluation and molecular docking simulations. *Bioorg. Med. Chem.* **2008**, *16*, 8072–8081.

(27) Cappelli, A.; Anzini, M.; Biava, M.; Makovec, F.; Giordani, A.; Caselli, G.; Rovati, L. C. 3-Substituted-1,5-diaryl-2-alkyl-pyrroles highly selective and orally effective COX-2 inhibitors. PCT Int. Appl. WO2008014821.

(28) Biava, M.; Porretta, G. C.; Poce, G.; De Logu, A.; Saddi, M.; Meleddu, R.; Manetti, F.; De Rossi, E.; Botta, M. 1,5-Diphenyl pyrrole derivatives as antimycobacterial agents. Probing the influence on antimycobacterial activity of lipophilic substituents at the phenyl rings. *J. Med. Chem.* **2008**, *51*, 3644–3648.

(29) Khanna, I. K.; Weier, R. M.; Paul, Y. Y.; Collins, W.; Miyashiro, J. M.; Koboldt, C. M.; Veenhuizen, A. W.; Currie, J. L.; Seibert, K.; Isakson, P. C. 1,2-Diarylpyrroles as potent and selective inhibitors of cyclooxygenase-2. *J. Med. Chem.* **1997**, *40*, 1619–1633.

(30) Anzini, M.; Canullo, L.; Braile, C.; Cappelli, A.; Gallelli, A.; Vomero, S.; Menziani, M. C.; De Benedetti, P. G.; Rizzo, M.; Collina, S.; Azzolina, O.; Sbacchi, M.; Ghelardini, C.; Galeotti, N. Synthesis, biological evaluation, and receptor docking simulations of 2-[(acylamino)ethyl]-1,4-benzodiazepines as κ-opioid receptor agonists endowed with antinociceptive and antiamnesic activity. *J. Med. Chem.* **2003**, *46*, 3853–3864.

(31) Ushiyama, S.; Yamada, T.; Murakami, Y.; Kumakura, S.; Inoue, S.; Suzuki, K.; Nakao, A.; Kawara, A.; Kimura, T. Preclinical pharmacology profile of CS-706, a novel cyclooxygenase-2 selective inhibitor, with potent antinociceptive and anti-inflammatory effects. *Eur. J. Pharmacol.* **2008**, *578*, 76–86.

(32) Gierse, J. K.; Zhang, Y.; Hood, W. F.; Walker, M. C.; Trigg, J. S.; Maziasz, T. J.; Koboldt, C. M.; Muhammad, J. L.; Zweifel, B. S.; Masferrer, J. L.; Isakson, P. C.; Seibert, K. Valdecoxib: Assessment of cyclooxygenase-2 potency and selectivity. *J. Pharmacol. Exp. Ther.* **2005**, *312*, 1206–1212.
(33) Esser, R.; Berry, C.; Du, Z.; Dawson, J.; Fox, A.; Fujimoto, R. A.; Haston, W.; Kimble, E. F.; Koehler, J.; Peppard, J.; Quadros, E.; Quintavalla, J.; Toscano, K.; Urban, L.; van Duzer, J.; Zhang, X.; Zhou, S.; Marshall, P. J. Preclinical pharmacology of lumiracoxib: A novel selective inhibitor of cyclooxygenase-2. *Br. J. Pharmacol.* **2005**, *144*, 538–550.
(34) Khanapure, S. P.; Garvey, D. S.; Young, D. V.; Ezawa, M.; Earl, R. A.; Gaston, R. D.; Fang, X.; Murty, M.; Martino, A.; Shumway, M.; Trocha, M.; Marek, P.; Tam, S. W.; Janero, D. R.; Letts, L. G. Synthesis and structure-activity relationship of novel, highly potent metharyl and methcycloalkyl cyclooxygenase-2 (COX-2) selective inhibitors. *J. Med. Chem.* **2003**, *46*, 5484–5504.
(35) Paramashivappa, R.; Kumar, P. P.; Rao, P. V. S.; Rao, A. S. Design, synthesis and biological evaluation of benzimidazole/benzothiazole and benzoxazole derivatives as cyclooxygenase inhibitors. *Bioorg. Med. Chem. Lett.* **2003**, *13*, 657–660.
(36) Warner, T. D.; Giuliano, F.; Vojnovic, I.; Bukasa, A.; Mitchell, J. A.; Vane, J. R. Nonsteroid drug selectivities for cyclo-oxygenase-1 rather than cyclo-oxygenase-2 are associated with human gastrointestinal toxicity: A full in vitro analysis. *Proc. Natl. Acad. Sci. U.S.A.* **1999**, *96*, 7563–7568.
(37) Tegeder, I.; Lötsch, J.; Krebs, S.; Muth-Selbach, U.; Brune, K.; Geisslinger, G. Comparison of inhibitory effects of meloxicam and diclofenac on human thromboxane biosynthesis after single doses and at steady state. *Clin. Pharmacol. Ther.* **1999**, *65*, 533–544.
(38) Meller, S. T.; Dykstra, C.; Grzybycki, D.; Murphy, S.; Gebhart, G. F. The possible role of glia in nociceptive processing and hyperalgesia in the spinal cord of the rat. *Neuropharmacology* **1994**, *33*, 1471–1478.
(39) Zingarelli, B.; Southan, G. J.; Gilad, E.; O'Connor, M.; Salzman, A. L.; Szabó, C. The inhibitory effects of mercaptoalkylguanidines on cyclo-oxygenase activity. *Br. J. Pharmacol.* **1997**, *120*, 357–366.
(40) Vaught, J.; Pelley, K.; Costa, L. G.; Sether, P.; Enna, S. J. A comparison of the antinociceptive responses to GABA-receptor agonists THIP and baclofen. *Neuropharmacology* **1985**, *24*, 211–216.
(41) Randal, L. O.; Selitto, J. J. A method for measurement of analgesic activity on inflamed tissue. *Arch. Int. Pharmacodyn. Ther.* **1957**, *111*, 409–419.